ACS Chemical Neuroscience

Research Article

pubs.acs.org/chemneuro

Non-Amyloid-β Component of Human α-Synuclein Oligomers Induces Formation of New Aβ Oligomers: Insight into the Mechanisms That Link Parkinson's and Alzheimer's Diseases

Yoav Atsmon-Raz[†,‡] and Yifat Miller*[,†,‡]

[†]Department of Chemistry, [‡]Ilse Katz Institute for Nanoscale Science and Technology, Ben-Gurion University of the Negev, Beer-Sheva 84105, Israel

Supporting Information

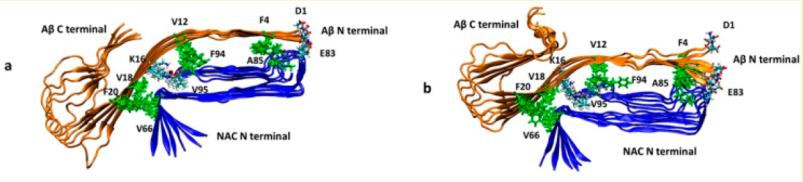

ABSTRACT: Parkinson's disease (PD) is characterized by the formation of Lewy bodies (LBs), of which their major component is the non-amyloid-β component (NAC) of α-synuclein (AS). Clinical studies have identified a link between PD and Alzheimer's disease (AD), but the question of why PD patients are at risk to develop various types of dementia, such as AD, is still elusive. *In vivo* studies have shown that Aβ can act as a seed for NAC/AS aggregation, promoting NAC/AS aggregation and thus contributing to the etiology of PD. However, the mechanisms by which NAC/AS oligomers interact with Aβ oligomers are still elusive. This work presents the interactions between NAC oligomers and Aβ oligomers at atomic resolution by applying extensive molecular dynamics simulations for an ensemble of cross-seeded NAC−Aβ_{1-42} oligomers. The main conclusions of this study are as follows: first, the cross-seeded NAC−Aβ_{1-42} oligomers represent polymorphic states, yet NAC oligomers prefer to interact with Aβ_{1-42} oligomers to form double-layer over single-layer conformations due to electrostatic/hydrophobic interactions; second, among the single-layer conformations, the NAC oligomers induce formation of new β-strands in Aβ_{1-42} oligomers, thus leading to new Aβ oligomer structures; and third, NAC oligomers stabilize the cross-β structure of Aβ oligomers, i.e., yielding compact Aβ fibril-like structures.

KEYWORDS: *Parkinson's disease, NAC, amyloids, self-assembly, peptides, cross-seeding, Alzheimer's disease, amyloid β, α-synuclein*

Parkinson's disease (PD) is characterized by the formation of neurotoxic, insoluble aggregates that are known as Lewy bodies (LBs), which are localized at the subcortical regions of the human brain. The major component of these insoluble aggregates is the non-amyloid-β component (NAC) of α-synuclein (AS).[1−8] The aggregation process of AS into LBs can also be observed in other neurodegenerative diseases, such as Parkinson's disease dementia (PDD), dementia with Lewy bodies (DLB), Lewy body variant of Alzheimer's disease (LBVAD), Guam-Parkinson-ALS dementia complex,[1,2] and Down's syndrome.[3] Interestingly, in some pathologies cases, aggregation of AS into LBs is observed in Alzheimer's disease (AD), which is primarily related to the aggregation of amyloid β (Aβ) peptides that form amyloids plaques[4−7] and Tau proteins[8] that form neurofibrillary tangles (NFTs).[9,10]

Recent studies have suggested that some PD patients share histopathological symptoms with those of Alzheimer's disease (AD) patients,[11] such as the formation of amyloid plaques[12] and NFTs[8] in addition to the formation of LBs. A link between PD and AD has been identified from clinical studies, which have shown that PD patients have an elevated risk of developing dementia (which is a primary symptom of AD as well) over non-PD patients.[6,7,11,13,14] Interestingly, other studies have shown that 50% of AD patients also have LBs present at autopsy.[3,9,15,16] Yet, the link between PD and AD and the question of why PD patients are at risk of developing various types of dementia, such as AD, are still elusive.

Both *in vitro*[12] and *in vivo*[17] studies have shown that Aβ has an inductive effect on the oligomerization of AS and that sonicated Aβ_{42} and Aβ_{40} can act as seeds for the aggregation of AS fibrils.[18] Furthermore, *in vitro* binding assays have shown that monomers of Aβ bind to residues E57−K97 of AS.[19] Interestingly, the sequence E57−K97 overlaps with the NAC domain, which is located at residues E61−V95 of AS, thus indicating direct binding between Aβ and NAC.[19] Recently, such binding between the AS monomer and Aβ monomer had been described as a heterodimer in atomic detail while using modified α-helical structures of monomeric forms of AS and Aβ.[20] This study also showed that Aβ monomer binds to the NAC domain in the AS monomer.[20] Yet, the toxic β-sheet-rich oligomers that initiate the formation of amyloid plaques from

Received: July 31, 2015
Revised: October 18, 2015
Published: October 19, 2015

DOI: 10.1021/acschemneuro.5b00204
ACS Chem. Neurosci. 2016, 7, 46−55

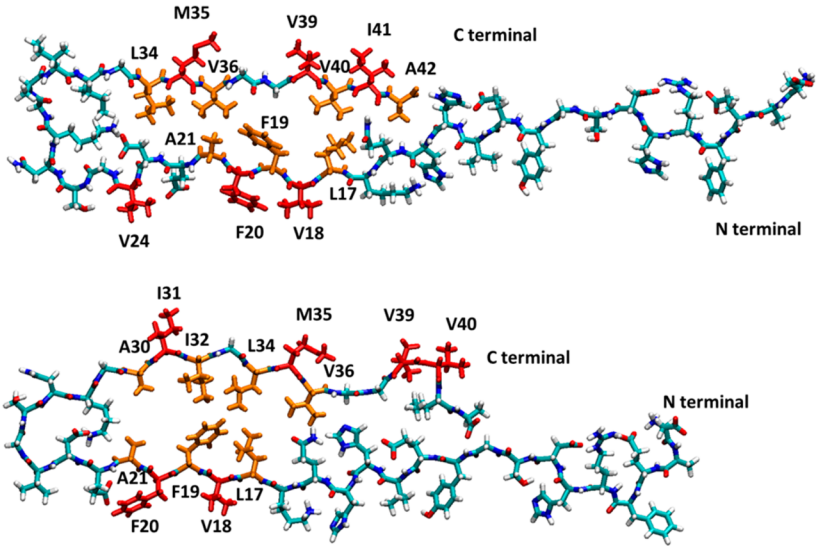

Figure 1. Extended monomer structures of Aβ_{1-42} based on (a) Aβ_{17-42}[39] and (b) Aβ_{9-40}.[40] Residues in orange illustrate the expected hydrophobic interactions in the inner core of Aβ. Residues in red show the hydrophobic interactions of Aβ that may interact with NAC to form double-layer conformations.

Aβ[21−25] and lead to the formation of LBs from AS[26−29] have not been studied so far.

The β-sheet-rich amyloid oligomers form cross-β structures of aggregates, such as oligomers, protofilaments, protofibrils, and fibrils.[30] Among these aggregates, oligomers are known to be the neurotoxic species in most amyloids that are related to neurodegenerative diseases.[31−34] Elongation of the cross-β structure of amyloids can occur via two different pathways: (1) self-assembly of amyloids, i.e., formation from a single type of amyloid, or (2) cross-seeding assembly of amyloids, i.e., formation of oligomers from two types of structurally similar amyloids.[35] Studies of the molecular interactions at atomic resolution of the self-assembly process of amyloids and the cross-seeding assembly process are essential in order to identify new pharmaceutical targets for neurodegenerative diseases such as AD and PD. Experimental investigations of cross-seeding between amyloids to identify the molecular interactions at atomic resolution present a considerable challenge. However, recent computational efforts have been performed to identify the interactions between two types of amyloids using molecular dynamics (MD) simulations: Aβ−WT tau's R2/R3/R4 repeat oligomers,[36] Aβ−ΔK280 mutated Tau R2 oligomers,[37] and amylin−Aβ oligomers.[38]

In this study, we present the first study of cross-seeded NAC−Aβ oligomers at atomistic resolution. Although the structure of Aβ oligomers has been solved experimentally,[39,40] the structure of NAC oligomers has not. Recently, we proposed a 3D structure for NAC oligomers using extensive MD simulations and compared them with available experimental parameters.[41] In this study, we applied our NAC oligomers[41] to form cross-seeded assemblies with previously determined Aβ oligomers from solid-state NMR (ssNMR) models of the Riek and Tycko groups.

Our simulations have shown that the cross-seeding between NAC and Aβ oligomers favors the formation of double-layer conformations (i.e., axial) over single-layer conformations (i.e., longitudinal). The double-layer conformations demonstrate polymorphism, in which the NAC oligomers show a preference for interacting with Aβ oligomers that are based on the Riek model. Furthermore, our simulations illustrated that in the cross-seeded NAC−Aβ oligomers the NAC oligomers changed the inner core distance of Aβ oligomers. In some cases, the NAC oligomers lead to the formation of well-packed β-cross fibril-like structures of Aβ, and in other cases, the NAC oligomers destabilize the cross-β structure of Aβ. Finally, the NAC oligomers induce formation of new β-strands in Aβ_{1-42} oligomers that are based on Riek's and Tycko's models, thus leading to new structures of Aβ oligomers. Therefore, this is the first study that shows new structures of Aβ oligomers that are produced due to their interactions with NAC oligomers.

RESULTS AND DISCUSSION

Constructed Models of NAC−Aβ Oligomers. The size of the oligomers was chosen based on previous studies that illustrated that the minimum number of amyloid monomers that are necessary for the formation of fibrils in prions is six.[42] We have constructed hexamers of NAC using the coordinates of the six monomers from our previously simulated NAC dodecamer (of model L11)[41] while excluding the monomers at each end of the dodecamer (Figure S1). For the construction of full-length Aβ_{1-42} hexamers (Figure S2), we applied the PDB structures that were reported from ssNMR experiments for Aβ_{17-42}[39] by the Riek group and for Aβ_{9-40}[40] by the Tycko group (Figure 1). We then extended the N-termini of Aβ_{17-42} by adding residues D1−K16 with the backbone dihedral angle values of β-strands (Figure 1a). Similarly, we extended the N-termini of Aβ_{9-40} by adding residues D1−S8, and we extended the C-termini by adding residues I41 and A42 (Figure 1b). We note that we have modified the backbone dihedral angles of residue V40 in Aβ_{9-40} to avoid clashes between residues I41 and A42 with the adjacent E11 (Figure 1b). Each of the extended Aβ_{1-42} monomers was then replicated into hexamers with a 5 Å spacing between the monomers.

For the initial comparison and evaluation of the structural similarity between NAC and Aβ, we applied the AsignMe package.[43−45] The AsignMe package allowed us to design a single-layer NAC−Aβ conformation while maximizing the similarity and identity of hydrophobic residues along the sequence of each type of amyloid (Figure S3). An additional single-layer NAC−Aβ conformation was designed by inverting

DOI: 10.1021/acschemneuro.5b00204
ACS Chem. Neurosci. 2016, 7, 46−55

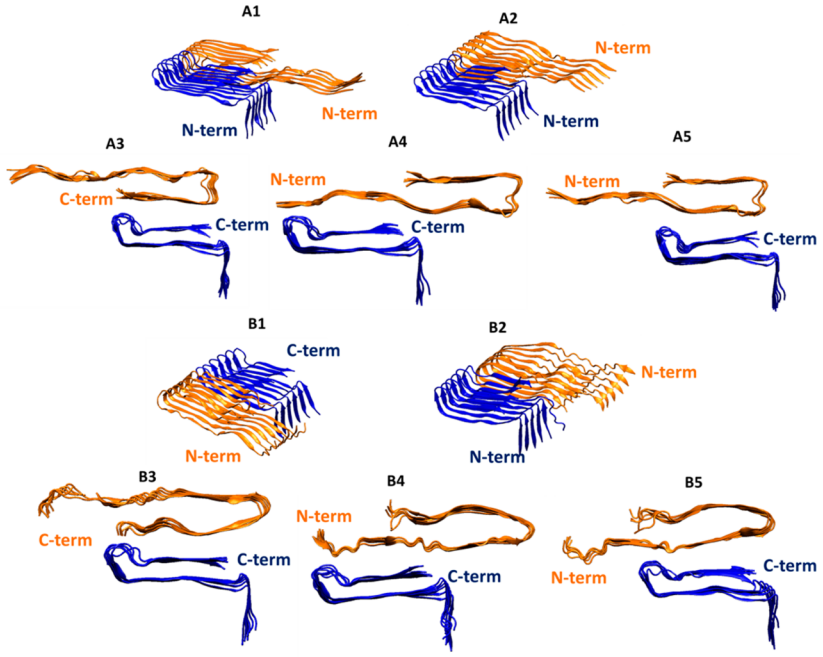

Figure 2. Initial constructed models of NAC−Aβ oligomers: NAC−Aβ oligomers in which Aβ oligomers are based on the Riek model[39] of Aβ: models A1−A5. NAC−Aβ oligomers in which Aβ oligomers are based on the Tycko model[40] of Aβ: models B1−B5. The NAC oligomers are based on our previous study.[41] Aβ oligomers are orange, and NAC oligomers blue.

the sequence of Aβ and comparing it with the NAC sequence using the AsignMe package (Figure S3).[43−45] These analyses illustrated the high identity and similarity of hydrophobic residues along the sequence of the two types of amyloids as well as their similar secondary structures. Finally, in the constructed single-layer NAC−Aβ conformations, we considered the maximum hydrogen-bond interactions between monomers within $A\beta_{1-42}$ oligomers, between monomers within NAC oligomers, and between one monomer of $A\beta_{1-42}$ and one monomer of the NAC oligomer.

In our previous study of the mutated Tau R2 repeat-Aβ oligomers, we constructed four different double-layer conformations by considering all of the possible interactions between these two amyloids that have β-arch structures (i.e., two β-strands connected by a turn region).[37] However, the NAC oligomer consists of three β-strands connected by two turn regions, whereas the third β-strand is located in the N-terminus of the NAC oligomer and thus cannot allow efficient interaction with Aβ to take place.[41] Therefore, only three possible double-layer NAC−Aβ conformations allow interactions to take place between the N-terminus of the NAC oligomer and the C- and N-termini of Aβ: one conformation with the C-terminus of Aβ and two conformations with the N-terminus of Aβ (Figure 2 and Table 1).

To examine the constructed single- and double-layer conformations, we considered the maximum molecular interactions accounting for salt-bridge and hydrophobic interactions between NAC oligomers and Aβ oligomers. We examined a total of five different structural orientations for the NAC−Aβ oligomers, in which Aβ oligomers are based on the Riek model (A1−A5) and five NAC−Aβ oligomers in which the Aβ oligomers are based on the Tycko model (B1−B5). Therefore, we have simulated a total of 10 NAC−Aβ oligomers (Figure S4). Specifically, the orientations between NAC oligomers and Aβ oligomers that were considered in this study are (1) a single-layer parallel conformation with the C-termini of NAC facing the C-termini of Aβ (A1/B1), (2) a single-layer parallel conformation with the C-termini of NAC facing the N-termini of Aβ (A2/B2), (3) a double-layer conformation in which the C-termini side chains of NAC oligomers face the C-termini side chains of $A\beta_{42}$ (A3/B3), (4) a double-layer conformation in which the C-termini of NAC oligomers face the N-termini of $A\beta_{42}$ (A4/B4) (for A4, Aβ D1−H14/NAC E83−V95; for B4, Aβ D1−H14/NAC E83−V95), and (5) a double-layer conformation in which the C-termini of NAC oligomers facing the N-termini of $A\beta_{42}$ (for A4, Aβ H14−S26/NAC E83−V95; for B4, Aβ E11−D23/NAC E83−V95) (A5/B5).

Table 1. Ten $A\beta_{1-42}$−NAC Dodecamer Models Investigated[a]

model	single/double layer	orientation between NAC and Aβ
A1	single	NAC N-terminal parallel to Aβ N-terminal
A2	single	NAC N-terminal parallel to Aβ C terminal
A3	double	C-terminal (NAC)−C-terminal (Aβ)
A4	double	C terminal (NAC)−N-terminal (Aβ)
A5	double	C-terminal (NAC)−N-terminal (Aβ)
B1	single	NAC N-terminal parallel to Aβ N-terminal
B2	single	NAC N-terminal parallel to Aβ C-terminal
B3	double	C-terminal (NAC)−C-terminal (Aβ)
B4	double	C-terminal (NAC)−N-terminal (Aβ)
B5	double	C-terminal (NAC)−N-terminal (Aβ)

[a]NAC−Aβ oligomers in which Aβ oligomers are based on the Riek model[39] of Aβ: models A1−A5. NAC−Aβ oligomers in which Aβ oligomers are based on the Tycko model[40] of Aβ: models B1−B5. The NAC oligomers are based on our previous study.[41]

NAC Oligomers Prefer To Interact with Aβ Oligomers To Form Double- over Single-Layer Conformations. Some of the most interesting questions related to cross-amyloid interactions include the following: (1) What are the forces that lead the two types of amyloids to interact? (2) What are the mechanisms by which the two types of amyloids interact with

DOI: 10.1021/acschemneuro.5b00204
ACS Chem. Neurosci. 2016, 7, 46−55

each other? In order to provide answers to these questions, it is necessary to investigate the interactions between two types of amyloids at the atomic resolution. Herein, we examined a total of 10 models of NAC−Aβ_{1-42} oligomers (Figure 2): five constructed NAC−Aβ_{1-42} oligomers that differ in the orientation between the two types of the amyloids for each Aβ model.[39,40]

To examine these 10 various NAC−Aβ_{1-42} oligomers (models A1−A5 and B1−B5), we ran MD simulations. Interestingly, simulated model B5 illustrated an unstable structure of Aβ_{1-42} oligomers, i.e., a lack of cross-β structure of Aβ. Furthermore, the NAC oligomers were separated from the Aβ_{1-42} oligomers, i.e., no cross-amyloid interactions appear in this model, probably due to electrostatic repulsion between the residues along the β-strands of each type of amyloid (Figure S5). Consequently, we have excluded this model from our study because it did not demonstrate cross-amyloid interactions.

We then estimated the conformational energies including the standard deviations of the nine simulated models using the GBMV method[46,47] (Table S1) and their populations using MC simulations. Figure 3 illustrates the populations of the nine

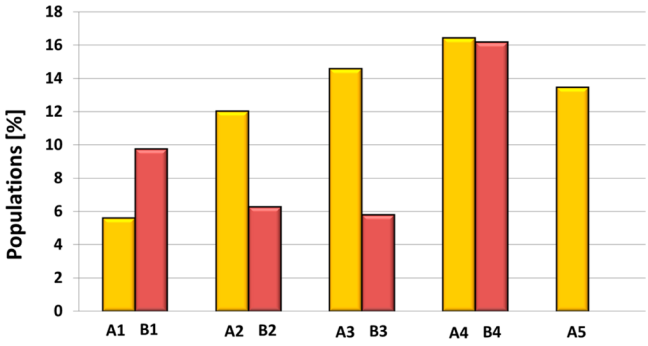

Figure 3. Populations of the simulated dodecamers of NAC−Aβ_{1-42} oligomers: Models A1−A5 (yellow) and models B1−B4 (red).

models of NAC−Aβ_{1-42} oligomers. It can be clearly seen in Figure 3 that models A3−A5, B3, and B4, which demonstrate double-layer conformations, have a higher percentage of populations compared to that for the four single-layer conformations (A1, A2, B1, and B2). One can compare the percentage of the total populations of the single-layer conformations to those of the double-layer conformations (Figure S6). Interestingly, one can see that the total percentage of populations for the double-layer conformations is twice that for the single-layer conformations. We therefore suggest that there is a strong preference for cross-amyloid interactions between NAC oligomers and Aβ_{1-42} oligomers that leads to the formation of double-layer conformations.

Interestingly, among all of the double-layer conformations of groups A3−A5 and B3−B4, models A4 and B4 show the highest percentage of populations; thus, we propose that the C-termini of NAC oligomers prefer to interact with the N-termini of Aβ_{1-42} oligomers. Both models A4 and B4 are characterized by three electrostatic interactions and three hydrophobic interactions (Figure 4). The first electrostatic interaction is between the amine group of the N-terminus of Aβ and the side chain of Glu83 of NAC, the second electrostatic interaction is along the fibril axis of Aβ, i.e., the amine group of the N-terminus of Aβ and the side chain of Asp1 of the adjacent Aβ, and the third electrostatic interaction is between Lys16 of Aβ

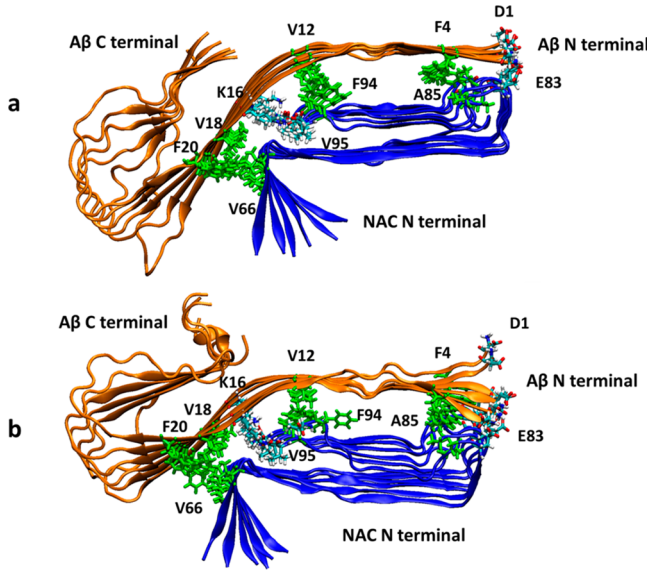

Figure 4. Electrostatic and hydrophobic interactions that stabilize NAC−Aβ_{1-42} oligomers in models A4 (a) and B4 (b). NAC oligomers are blue; and Aβ_{1-42} oligomers are orange.

and the carboxyl group of the C-terminus of NAC. Models A4 and B4 also share three hydrophobic interactions: Phe4 of Aβ and Ala85 of NAC, Val12 of Aβ and Phe94 of NAC, and Val18 and Phe20 of Aβ and Val66 of NAC. These interactions are uniquely dependent on the orientation between NAC and Aβ_{1-42}, as illustrated in models A4 and B4. We therefore propose that these interactions are the major driving forces behind the preference of these orientations among the other double-layer conformations that have been investigated in this study.

NAC Oligomers Induce Formation of New β-Strands in the Aβ Oligomers. One of the interesting issues that can be investigated in cross-amyloid interactions is the study of the effect of one type of self-assembled amyloid on the structure of the second type of self-assembled amyloid. Specifically, it is of great interest to learn how cross-amyloid interactions affect the secondary structure of the self-assembly of the two types of amyloids. In the initially constructed models of NAC−Aβ_{1-42} oligomers (Figure 2), the NAC oligomers were based on our previous structural model[41] and Aβ_{1-42} oligomers were based on the experimental ssNMR structural models of Riek (Aβ_{17-42})[39] and Tycko (Aβ_{9-40}).[40] While NAC oligomers consist of three β-strands connected by two turn regions, the two experimental ssNMR models of Aβ_{1-42} oligomers show that Aβ_{1-42} oligomers consist of two β-strands connected by one turn region. In the cross-seeded state, when NAC oligomers interact with Aβ_{1-42} oligomers, the secondary structure of NAC oligomers does not change, i.e., the NAC oligomer conserves the three β-strands connected by the two turn regions (Figure 5). However, the secondary structure of Aβ_{1-42} oligomers of both Tycko's and Riek's models in the cross-seeded state has changed during the simulations: the Aβ_{1-42} oligomers of Tycko's model consist of three β-strands connected by two turn regions, and Riek's models consist of four β-strands connected by three turn regions (Figure 6). We therefore suggest that NAC oligomers induce the formation of new Aβ oligomers.

The ssNMR model of Riek for Aβ_{17-42}[39] illustrates two β-strands located at residues 17−21 and 28−42 connected by a

DOI: 10.1021/acschemneuro.5b00204
ACS Chem. Neurosci. 2016, 7, 46−55

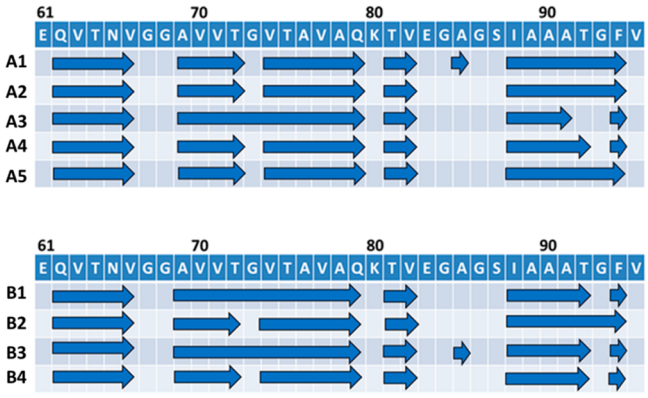

Figure 5. Secondary structures of the NAC−Aβ oligomers of models A1−A5 and B1−B4.

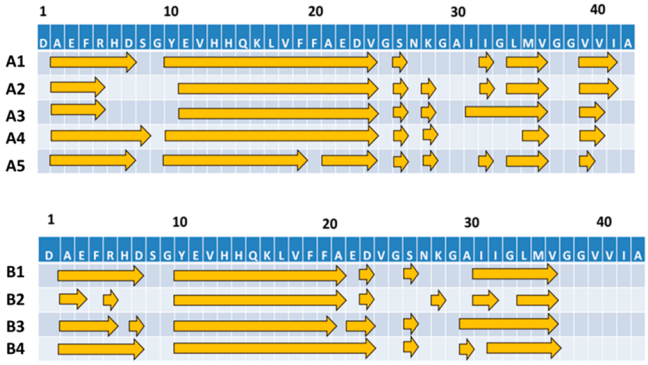

Figure 6. Secondary structures of the Aβ oligomers in the NAC−Aβ oligomers of models A1−A5 and B1−B4. Models A1−A5 consist of four β-strands, and models B1−B4 consist of three β-strands.

turn, which is located at residues 22−27. The ssNMR model of Tycko for $A\beta_{9-40}$[40] also suggests two β-strands (residues 9−24 and 32−40) and a turn located at 25−31. Both ssNMR studies suggested that the N-termini are structurally disordered. However, in our previous studies,[36,48,49] we extended the N-termini of the isolated $A\beta_{1-42}$ oligomers for these two ssNMR models and simulated these structures. Our simulations showed that the extension of the N-termini led to the extension of the first β-strand with no formation of a new β-strand or a new turn region in the N- or C-terminal parts.

Applying the AsignMe package, we showed that the sequences of NAC oligomers and $A\beta_{1-42}$ share high similarity and identity, which is also the case for their secondary structures. Interestingly, one can see that the new turn regions in the Aβ oligomers of the cross-seeded oligomers consist of glycine residues, which are also positioned in the turn regions of both in cross-seeded NAC as illustrated here and in the NAC oligomers which we previously illustrated in the self-assembled NAC oligomer.[50] Previous studies showed that glycine residues have the tendency to be localized at loop/turn regions of peptides and proteins.[51,52] Therefore, in the cross-seeded NAC−$A\beta_{1-42}$ oligomers, the glycine residues along the sequence of NAC that are located in the turn regions affect the formation of new turns/loops in $A\beta_{1-42}$ that also consist of glycine residues along the sequence. Consequently, new β-strands are formed in $A\beta_{1-42}$. We have previously shown that Aβ oligomers that were originally based on Tycko's model consist of three β-strands connected by two turn regions (and not two β-strands connected by one turn region, as expected in the original experiment-based Aβ oligomers) in cross-seeded amylin−$A\beta_{1-42}$ oligomers.[53] The new third β-strand in the cross-seeded amylin−$A\beta_{1-42}$ oligomers is located in residues Val39−Ala42 in the C-termini of $A\beta_{1-42}$. Here, in the cross-seeded NAC−$A\beta_{1-42}$ oligomers, in Tycko's model the new third β-strand is located in the N-terminus, residues Asp1−Asp7 (and the new second turn is located in residues Ser8−Gly9), as seen in Figure 6. Similarly, in the NAC−$A\beta_{1-42}$ oligomers, Riek's model of $A\beta_{1-42}$ also illustrates a new β-strand that is located in the N-terminus (residues Asp1−Asp7) and another shorter β-strand which is located in the C-terminus of $A\beta_{1-42}$ (residues Val39−Ala42). Residues Val39−Ala42 in the C-terminus of $A\beta_{1-42}$ of Tycko's model illustrate disordered regions that sterically disturb the interactions between Aβ monomers along the fibril axis and thus prevent the formation of a β-strand (Figure S7). However, these residues in Riek's model illustrate a β-strand that further stabilizes the structural stability of the cross-β structure in the cross-seeded fibrillary state. The stabilities of these β-strands were examined using RMSF (Figures S8 and S9) and RMSD (Figures S10 and S11) analyses.

Interestingly, analysis of the solvation of the residues of NAC oligomers (Figure 7) and Aβ oligomers (Figure 8) in cross-seeded states is in accordance with the secondary structure analysis. The domains that illustrate β-strands show relatively low solvation because of the hydrophobic residues that form hydrophobic cores. The turn/loop domains demonstrate

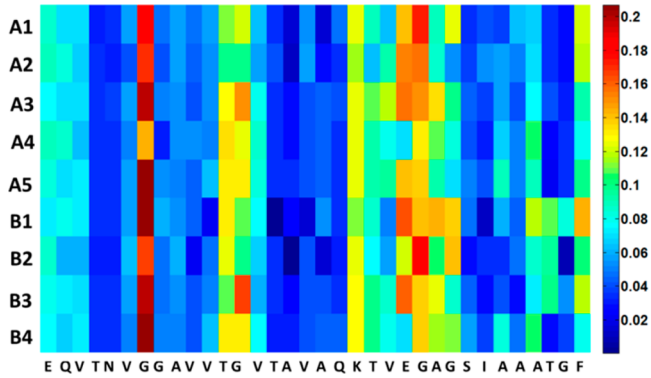

Figure 7. Average number of water molecules around each side chain Cβ carbon (within 4 Å) for the NAC oligomers in the simulated cross-seeded NAC−$A\beta_{1-42}$ oligomers.

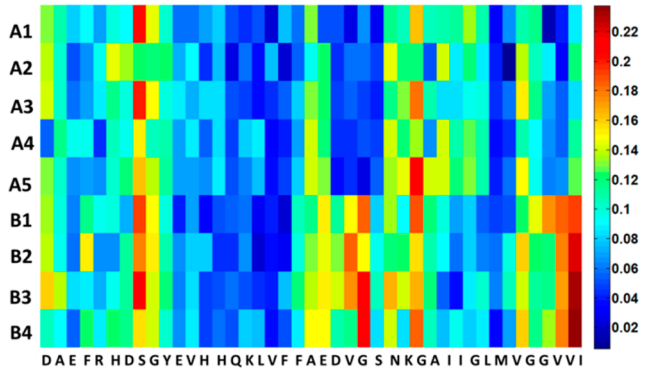

Figure 8. Average number of water molecules around each side chain Cβ carbon (within 4 Å) for the Aβ oligomers in the simulated cross-seeded NAC−Aβ oligomers.

DOI: 10.1021/acschemneuro.5b00204
ACS Chem. Neurosci. 2016, 7, 46−55

relatively high solvation, particularly the glycine residues in these domains, which are known to be less solvated residues. It is well-documented in the literature that amyloids form cross-β structures with hydrophobic cores and that the loops are relatively solvated and more exposed to solution.[54,55] This scenario is also seen here in the cross-seeded state of NAC−Aβ_{1-42} oligomers.

Inner Core Distances of Aβ Oligomers Are Changed Due to the Cross-Seeding NAC−Aβ Oligomers. Previously, we have shown that the inner core value of amylin and Aβ_{1-42} in cross-seeded amylin$_{1-37}$−Aβ_{1-42} oligomers is similar to those of the separated amylin oligomers and Aβ oligomers.[53] In other words, we proposed that there is no synergistic effect of the cross-seeding on the inner core of these two amyloids. Here, we present, for the first time, that one type of amyloid can change the inner core of the second type of amyloid in cross-seeding between two types of amyloids (Figure 9 and Table S2).

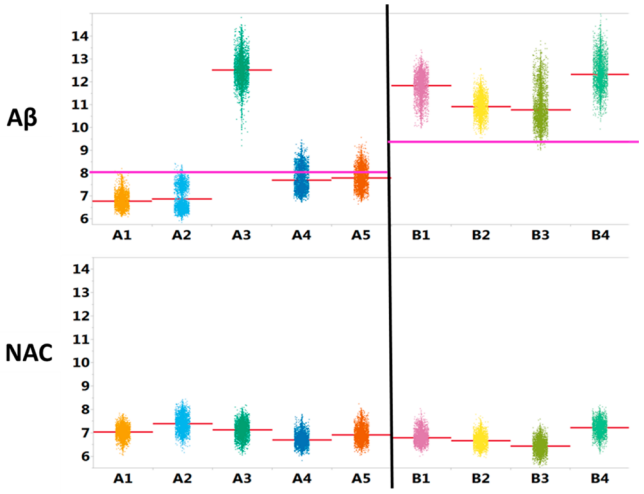

Figure 9. Cα−Cα backbone inner core distances for the simulated cross-seeded NAC−Aβ oligomers. Top left: The inner core distances (Ala21−Val36) of Aβ oligomers of models that are based on Riek's model. The pink line is the experiment-based inner core value of Aβ_{17-42}.[39] Top right: The inner core distances (Phe19−Ile32) of Aβ oligomers of models that are based on Tycko's model. The pink line is the experiment-based inner core value of Aβ_{9-40}.[40] Bottom left: The inner core distances of NAC oligomers of models that are based on Riek's model. Bottom right: The inner core distances of NAC oligomers of models that are based on Tycko's model. The red lines in all dotted clusters illustrate the robust mean values for each ensemble of measurements that were taken from the last 5 ns of each simulation.

The Riek group estimated the inner core distance (i.e., the distance between the Cα atoms of Ala21 and Val36) of Aβ_{17-42} to be 8.0 Å. We have measured this inner core distance of Aβ between the Cα atoms of Ala21 and Val36 for all of the cross-seeded NAC−Aβ_{1-42} models (A1−A5), which are based on the experimental model of Riek.[39] Interestingly, the inner core distances of Aβ in the single-layer conformations of cross-seeded models A1 and A2 were decreased to 6.8 and 6.9 Å, respectively (in comparison to the experiment-based model of Riek). Therefore, we propose that the NAC oligomers decrease the inner core distance of Aβ in the single-layer conformations, probably due to the hydrophobic interactions between these two types of amyloids. Previously, we illustrated that in cross-seeded Aβ−Tau repeat oligomers the Aβ oligomers decrease the inner core of some of the Tau repeat oligomers.[36] However, the inner core distances of Aβ in the double-layer conformations of cross-seeded models A4 and A5 were only slightly decreased to 7.8 Å and were strongly increased to 12.5 Å in model A3. Therefore, in the double-layer conformations in which the C-termini of NAC oligomers interact with the N-termini of Aβ (models A4 and A5), the NAC oligomers decrease the inner core of Aβ. In contrast, only in the case where the C-termini of NAC oligomers interact with the C-termini of Aβ does the NAC oligomer strongly increase the inner core distance. We therefore conclude that in most of the cross-seeded NAC−Aβ_{1-42} oligomers in which Aβ is based on the Riek model, the NAC oligomers stabilize the cross-β structure, forming strong contacts between β-strands.

The Tycko group has proposed that the inner core distance between the strands of Aβ_{9-40} is 9.5 Å, which was previously measured to be the distance between Cα atoms of Phe19 and Ile32 of Aβ.[56] Here, we measured this distance for models B1−B4. Interestingly, for all single- and double-layer conformations, the inner core distances of Aβ in the cross-seeded NAC−Aβ_{1-42} oligomers were increased (above 10 Å). We therefore suggest that in the cross-seeded NAC−Aβ_{1-42} oligomers, in which Aβ is based on Tycko's model, the NAC oligomers relatively destabilize the cross-β structure of Aβ.

Finally, we examined whether the inner core distance of NAC oligomer is affected by the cross-seeding between the NAC oligomer and each one of the Aβ oligomer models. Interestingly, the inner core distances of NAC oligomers in all models (A1−A5 and B1−B4) have not changed or changed only slightly (6.9 ± 0.3 Å; Table S2). We therefore conclude that each of the two experiment-based Aβ oligomers does not affect the cross-β packing of NAC oligomers.

CONCLUSIONS

AS protein is an amyloid that is related to PD, and Aβ peptide is an amyloid that is related to AD. The clinical relationship between these two diseases has been established for over a decade.[12,57] An earlier *in vitro* study has shown that the NAC domain in AS interacts with Aβ.[19] Recent experimental studies have illustrated the existence of cross-seeded NAC−Aβ oligomers,[19,58,59] but the interactions between these two types of amyloids at atomic resolution remain unknown. A recent computational study investigated the interactions between a monomer of AS and a monomer of Aβ.[20] This computational study has revealed that the hydrophobic NAC domain along the AS monomer strongly interacts with the Aβ monomer. Yet, it is well-known that the monomer of Aβ plays significant roles as an antioxidant[60] and as a neuroprotective agent[61] and that AS monomer plays important roles in maintaining a supply of synaptic vesicles in presynaptic terminals and regulating the release of dopamine, a type of neurotransmitter that is critical for controlling the starting and stopping of voluntary and involuntary movements.[62] However, AS oligomers and Aβ oligomers are toxic species, and they play a central role in amyloidosis. Currently, there is a lack of evidence in the literature for the structure of cross-seeded AS−Aβ oligomers at atomic resolution.

Since experimental evidence has shown that the NAC domain strongly interacts with Aβ[19] and that the hydrophobic NAC domain in AS shares a similar secondary structure with that of Aβ, we examined our NAC oligomers[50] to investigate the interactions between NAC and Aβ oligomers. The current work is the first study to illustrate the interactions between

DOI: 10.1021/acschemneuro.5b00204
ACS Chem. Neurosci. 2016, 7, 46−55

NAC and Aβ oligomers at atomic resolution. The NAC oligomers interacted using one of the two different ssNMR models of Aβ oligomers: Riek's model[39] and Tycko's model.[40]

Four conclusions can be drawn from this study. First, the cross-seeded NAC−Aβ oligomers demonstrate polymorphism. The NAC oligomers interact with Aβ oligomers (for both ssNMR models) in various conformations: single- and double-layer conformations. Polymorphism is a phenomenon that has been extensively reported in various amyloids, such as AS,[63,64] amylin,[50] Rep-WH1,[65] Tau,[66] and Aβ.[67,68] Our previous studies have suggested that cross-seeding two types of amyloids, such as mutated ΔK280 Tau R2−Aβ[37] and amylin−Aβ[53] oligomers, also demonstrate polymorphism. This work illustrates that the cross-seeded NAC−Aβ oligomers also represent polymorphic states with a rugged landscape potential.

Second, although NAC−Aβ oligomers exhibit polymorphism, analysis of the populations has shown that NAC oligomers prefer to interact with Aβ oligomers to form double- over single-layer conformations. Previously, we have illustrated that in ΔK280 Tau R2−Aβ oligomers the double-layer conformations are also preferred over single-layer conformations due to the electrostatic/hydrophobic interactions between the two types of amyloids.[37] These interactions are known to stabilize double-layer conformations that share a structural resemblance to the K18 and K19 tau octamers.[69] Interestingly, similar interactions that stabilize the double-layer conformation in which the N-termini of NAC oligomers interact with the C-termini of Aβ oligomers were observed for the two experimental-based models of Aβ oligomers, i.e., models A4 and B4 (Figure 4).

Third, in the cross-seeded NAC−Aβ oligomers, the self-assembled NAC oligomers that consist of three β-strands connected by two turn regions affect the secondary structure of the self-assembled Aβ oligomers. While the experimental-based structural models of Riek and Tycko for Aβ oligomers consist of two β-strands connected by one turn region, in the simulated cross-seeding NAC−Aβ oligomers, the Aβ oligomers that are based on Riek's model consist of four β-strands connected by three turn regions and those that are based on Tycko's model consist of three β-strands connected by two turn regions. Previously, we illustrated that the experiment-based structural model of Tycko for Aβ oligomers in the cross-seeded amylin−Aβ oligomers also demonstrates three β-strands connected by two turn regions.[53] We therefore propose that NAC oligomers (similarly to amylin oligomers) induce the formation of third and fourth β-strands in the cross-β structure of Aβ. Interestingly, a recent experiment-based structural model of Aβ oligomer by the Ishii group illustrated a new structure of Aβ oligomer that consists of three β-strand connected by two turn regions,[70] similar to what we observed for Aβ oligomers of Tycko's model in our previous study[53] and in the current study. We present here a new Aβ oligomer that consists of four β-strands connected by three turn regions that had been observed for the Aβ oligomers of Riek.

Fourth, in all cross-seeded NAC−$Aβ_{1-42}$ oligomers, the inner core distance values of NAC oligomers (between the two main longest β-strands) were not changed due to the interactions with Aβ oligomers. However, the inner core distances of the single-layer conformation of Aβ oligomers (both of Tycko's and Riek's models) were decreased (by ∼15%), forming a more compact stable cross-β structure due to the strong hydrophobic interactions in the inner core domain.

The current study is focused on the coassembly pathway of NAC and $Aβ_{1-42}$ when either species is in its stable self-assembled structure, i.e., preformed oligomeric states. Our study shows that the coaggregation of NAC and $Aβ_{1-42}$ is thermodynamically feasible. It is important to note that other aggregation pathways of NAC and $Aβ_{1-42}$ can also be feasible, such as disordered aggregates of both NAC and $Aβ_{1-42}$ or aggregates with interspersed NAC and $Aβ_{1-42}$ units. Future work needs to consider other coaggregation pathways of NAC and $Aβ_{1-42}$.

Our current work may provide insight into the cross-seeding process between NAC and Aβ oligomers and thus provides insight into the link between PD and AD. One can suggest that in order to prevent patients with PD from developing AD or vice versa it is important to develop a drug that takes two strategies into consideration: (1) design a drug that will bind to NAC/AS oligomers in order to destabilize the cross-β structure of NAC/AS oligomers. Consequently, the NAC/AS oligomer will not stabilize Aβ oligomers and/or the cross-seeded NAC/AS-Aβ oligomers. Therefore, the drug will inhibit Aβ aggregation and/or the cross-seeding NAC/AS−Aβ aggregation. (2) Design small molecules that will interact with the β-strands of the two types of amyloids, NAC/AS and Aβ. Consequently, these molecules will inhibit the electrostatic/hydrophobic interactions between the NAC/AS and Aβ oligomers.

METHODS

Molecular Dynamics (MD) Simulations Protocol. We constructed the models of NAC, Aβ, and NAC−Aβ oligomers using Accelerys Discovery Studio software (http://accelrys.com/products/discovery-studio/). MD simulations of the solvated oligomers were performed in the NPT ensemble using NAMD[71] with the CHARMM27 force field.[72,73] The dodecamers were energy minimized and explicitly solvated in a TIP3P[74,75] water box with a minimum distance of 15 Å from each edge of the box. All water molecules within 2.5 Å of the dodecamers were removed. Counter ions were added at random locations to neutralize the charge on the dodecamers. The Langevin piston method[71,76,77] with a decay period of 100 fs and a damping time of 50 fs was used to maintain a constant pressure of 1 atm. The temperature was controlled at 330 K by a Langevin thermostat with a damping coefficient of 10 ps.[71] Short-range van der Waals (vdW) interactions were calculated using the switching function, with a twin range cutoff of 10.0 and 12.0 Å. Long-range electrostatic interactions were calculated using the particle mesh Ewald method with a cutoff of 12.0 Å.[78,79] The equations of motion were integrated using the leapfrog integrator with a step of 1 fs. The solvated systems were energy minimized for 2000 conjugated gradient steps, where the hydrogen-bonding distance between the β-sheets of each dodecamer was fixed in the range 2.2−2.5 Å.

The counterions and water molecules were allowed to move. The hydrogen atoms were constrained to the equilibrium bond by using the SHAKE algorithm.[80] The minimized solvated systems were energy minimized for 5000 additional conjugate gradient steps and 20 000 heating steps at 250 K, with all atoms being allowed to move. Then, the system was heated from 250 to 330 K for 300 ps and equilibrated at 330 K for 300 ps. We ran simulations at a higher temperature than physiological (310 K), with the aim of investigating the stability of the constructed models. Obviously, structures that are stable at 330 K will be also stable at lower temperatures. All simulations were run for 60 ns. These conditions were applied to test the stability of all constructed models.

Structural Analysis Details. We examined the structural stability of the studied oligomers by following the changes in the number of hydrogen bonds between β-strands, with the hydrogen-bond cutoff being set at 2.5 Å. Further structural analysis was performed by computing the root-mean square deviations (RMSDs) and root-mean

DOI: 10.1021/acschemneuro.5b00204
ACS Chem. Neurosci. 2016, 7, 46−55

square fluctuations (RMSFs) and by monitoring the strand-to-strand distance in each monomer of each simulated oligomer. We monitored this distance by considering the distance between the Cα atoms of Ala21 and Val36 for models A1−A5 of NAC−Aβ oligomers, whereas for models B1−B4 of NAC−Aβ oligomers, we considered the distance between the Cα atoms of Phe19 and Ile32. For all models (A1−A5, B1−B4), the strand-to-strand distance of NAC was chosen as the distance between the Cα atoms of Thr75 and Ala89. The inner core distance for each oligomer was evaluated by measuring the aforementioned distances for all of its monomers and averaging their values while excluding the terminal monomers.

Secondary Structure Analysis. The location of the β-strands was determined for each model by computing the dihedral angles Ψ and Φ of the last 5 ns for each residue along both the Aβ and NAC oligomers. The ranges of −60 to −160° and 90 to 170° were, respectively, defined as the allowed values for Φ and Ψ that define a β-sheet structure.[81]

Generalized Born Method with Molecular Volume (GBMV). To obtain the relative conformational energies of the studied oligomers, the oligomer trajectories of the last 5 ns were first extracted from the explicit MD simulation excluding water molecules. The solvation energies of all systems were calculated using the generalized Born method with molecular volume (GBMV).[46,47] In the GBMV calculations, the dielectric constant of water was set to 80. The hydrophobic solvent-accessible surface area (SASA) term factor was set to 0.005 92 kcal/(mol Å^2). Each conformer was minimized using 1000 cycles, and the conformational energy was evaluated by grid-based GBMV.

A total of 4500 conformations (500 conformations for each of the nine examined NAC−Aβ oligomers) and 1000 conformations (500 conformations for each of the two examined Aβ oligomers) were used to construct the energy landscape of the NAC−Aβ oligomers and to evaluate the conformer probabilities by using Monte Carlo (MC) simulations. In the first step, one conformation of conformer i and one conformation of conformer j are randomly selected. Then, the Boltzmann factor is computed as $e^{-(E_j-E_i)/KT}$, where E_i and E_j are the conformational energies evaluated using the GBMV calculations for conformations i and j, respectively, K is the Boltzmann constant, and T is the absolute temperature (298 K used here). If the Boltzmann factor value is larger than the random number, then the move from conformation i to conformation j is allowed. After 10^6 steps, the conformations visited for each conformer were counted. Finally, the relative probability of conformer n was evaluated as $P_n = N_n/N_{total}$, where P_n is the population of conformer n, N_n is the total number of conformations visited for conformer n, and N_{total} is the total steps. The advantages of using the MC simulations to estimate conformer probability rely on the facts that the MC simulations have good numerical stability and allow transition probabilities among several conformers to be controlled.

Using all nine conformers and 4500 conformations of the NAC−Aβ oligomers generated from the MD simulations, we estimated the overall stability and populations for each conformer based on the MD simulations with the energy landscape computed with GBMV for all conformers. For the complex kinetics of amyloid formation, this group is likely to represent only a very small percentage of the ensemble. Nevertheless, the carefully selected models cover the most likely structures. To compare the result of the relative conformational energies obtained from GBMV method, we used Origin Pro[21] to analyze the distribution of the conformational energies (Tables S1). All 500 values of each conformer extracted from the last 5 ns of the simulations were used to characterize the distribution by histograms with a bin width of 50 kcal/mol. A single peak Gaussian function was chosen for each simulation. This allowed us to extract the mean and standard deviation of the solvation energies for each model that we constructed and simulated.

■ ASSOCIATED CONTENT

Supporting Information

The Supporting Information is available free of charge on the ACS Publications website at DOI: 10.1021/acschemneuro.5b00204.

Simulated structures of NAC hexamer, $A\beta_{1-42}$ hexamers, and NAC−$A\beta_{1-42}$ dodecamers; alignments and probabilities of β-sheet formation for NAC and $A\beta_{1-42}$ using AlignMe; interactions between NAC oligomer and $A\beta_{1-42}$ oligomer of model B5; structural analysis (RMSD and RMSF) of the simulated cross-seeded NAC−$A\beta_{1-42}$ oligomers; and detailed population analysis and conformational energies of the simulated NAC−$A\beta_{1-42}$ oligomers (PDF)

■ AUTHOR INFORMATION

Corresponding Author

*E-mail: ymiller@bgu.ac.il.

Funding

This project was supported by the FP7-PEOPLE-2011-CIG Marie Curie Career Integration Grant, research grant no. 303741.

Notes

The authors declare no competing financial interest.

■ ACKNOWLEDGMENTS

All simulations were performed using the high-performance computational facilities of the Miller Lab in BGU HPC computational center. The support of the BGU HPC computational center staff is greatly appreciated.

■ REFERENCES

(1) Forman, M. S., Schmidt, M. L., Kasturi, S., Perl, D. P., Lee, V. M., and Trojanowski, J. Q. (2002) Tau and alpha-synuclein pathology in amygdala of Parkinsonism-dementia complex patients of Guam. *Am. J. Pathol. 160* (5), 1725−31.

(2) Lippa, C. F., Fujiwara, H., Mann, D. M., Giasson, B., Baba, M., Schmidt, M. L., Nee, L. E., O'Connell, B., Pollen, D. A., St. George-Hyslop, P., Ghetti, B., Nochlin, D., Bird, T. D., Cairns, N. J., Lee, V. M., Iwatsubo, T., and Trojanowski, J. Q. (1998) Lewy bodies contain altered alpha-synuclein in brains of many familial Alzheimer's disease patients with mutations in presenilin and amyloid precursor protein genes. *Am. J. Pathol. 153* (5), 1365−70.

(3) Lippa, C. F., Schmidt, M. L., Lee, V. M., and Trojanowski, J. Q. (1999) Antibodies to alpha-synuclein detect Lewy bodies in many Down's syndrome brains with Alzheimer's disease. *Ann. Neurol. 45* (3), 353−7.

(4) Schmechel, D. E., Saunders, A. M., Strittmatter, W. J., Crain, B. J., Hulette, C. M., Joo, S. H., Pericak-Vance, M. A., Goldgaber, D., and Roses, A. D. (1993) Increased amyloid beta-peptide deposition in cerebral cortex as a consequence of apolipoprotein E genotype in late-onset Alzheimer disease. *Proc. Natl. Acad. Sci. U. S. A. 90* (20), 9649−9653.

(5) Walsh, D., Klyubin, I., Fadeeva, J., Rowan, M., and Selkoe, D. (2002) Amyloid-beta oligomers: their production, toxicity and therapeutic inhibition. *Biochem. Soc. Trans. 30* (4), 552−557.

(6) Hurtig, H. I., Trojanowski, J. Q., Galvin, J., Ewbank, D., Schmidt, M. L., Lee, V. M., Clark, C. M., Glosser, G., Stern, M. B., Gollomp, S. M., and Arnold, S. E. (2000) Alpha-synuclein cortical Lewy bodies correlate with dementia in Parkinson's disease. *Neurology 54* (10), 1916−21.

(7) Leverenz, J. B., Quinn, J. F., Zabetian, C., Zhang, J., Montine, K. S., and Montine, T. J. (2009) Cognitive impairment and dementia in

DOI: 10.1021/acschemneuro.5b00204
ACS Chem. Neurosci. 2016, 7, 46−55

patients with Parkinson disease. *Curr. Top. Med. Chem. 9* (10), 903–12.
(8) Moussaud, S., Jones, D. R., Moussaud-Lamodiere, E. L., Delenclos, M., Ross, O. A., and McLean, P. J. (2014) Alpha-synuclein and tau: teammates in neurodegeneration? *Mol. Neurodegener. 9*, 43.
(9) Hamilton, R. L. (2000) Lewy Bodies in Alzheimer's Disease: A Neuropathological Review of 145 Cases Using α-Synuclein Immunohistochemistry. *Brain Pathol. 10* (3), 378–384.
(10) Ballatore, C., Lee, V. M., and Trojanowski, J. Q. (2007) Tau-mediated neurodegeneration in Alzheimer's disease and related disorders. *Nat. Rev. Neurosci. 8* (9), 663–72.
(11) Galpern, W. R., and Lang, A. E. (2006) Interface between tauopathies and synucleinopathies: A tale of two proteins. *Ann. Neurol. 59* (3), 449.
(12) Mandal, P. K., Pettegrew, J. W., Masliah, E., Hamilton, R. L., and Mandal, R. (2006) Interaction between Aβ peptide and α synuclein: molecular mechanisms in overlapping pathology of Alzheimer's and Parkinson's in dementia with Lewy body disease. *Neurochem. Res. 31* (9), 1153–1162.
(13) Aarsland, D., Zaccai, J., and Brayne, C. (2005) A systematic review of prevalence studies of dementia in Parkinson's disease. *Mov. Disord. 20* (10), 1255–63.
(14) Braak, H., Rub, U., Jansen Steur, E. N., Del Tredici, K., and de Vos, R. A. (2005) Cognitive status correlates with neuropathologic stage in Parkinson disease. *Neurology 64* (8), 1404–10.
(15) Leverenz, J. B., Fishel, M. A., Peskind, E. R., Montine, T. J., Nochlin, D., Steinbart, E., Raskind, M. A., Schellenberg, G. D., Bird, T. D., and Tsuang, D. (2006) Lewy body pathology in familial Alzheimer disease: evidence for disease- and mutation-specific pathologic phenotype. *Arch. Neurol. 63* (3), 370–6.
(16) Leverenz, J. B., Hamilton, R., Tsuang, D. W., Schantz, A., Vavrek, D., Larson, E. B., Kukull, W. A., Lopez, O., Galasko, D., Masliah, E., Kaye, J., Woltjer, R., Clark, C., Trojanowski, J. Q., and Montine, T. J. (2008) Empiric refinement of the pathologic assessment of Lewy-related pathology in the dementia patient. *Brain Pathol. 18* (2), 220–4.
(17) Masliah, E., Rockenstein, E., Veinbergs, I., Sagara, Y., Mallory, M., Hashimoto, M., and Mucke, L. (2001) beta-amyloid peptides enhance alpha-synuclein accumulation and neuronal deficits in a transgenic mouse model linking Alzheimer's disease and Parkinson's disease. *Proc. Natl. Acad. Sci. U. S. A. 98* (21), 12245–50.
(18) Spillantini, M. G., Crowther, R. A., Jakes, R., Hasegawa, M., and Goedert, M. (1998) α-Synuclein in filamentous inclusions of Lewy bodies from Parkinson's disease and dementia with Lewy bodies. *Proc. Natl. Acad. Sci. U. S. A. 95* (11), 6469–6473.
(19) Jensen, P. H., Hojrup, P., Hager, H., Nielsen, M. S., Jacobsen, L., Olesen, O. F., Gliemann, J., and Jakes, R. (1997) Binding of Abeta to alpha- and beta-synucleins: identification of segments in alpha-synuclein/NAC precursor that bind Abeta and NAC. *Biochem. J. 323* (2), 539–546.
(20) Jose, J. C., Chatterjee, P., and Sengupta, N. (2014) Cross dimerization of amyloid-beta and alphasynuclein proteins in aqueous environment: a molecular dynamics simulations study. *PLoS One 9* (9), e106883.
(21) Selkoe, D. J. (2001) Alzheimer's disease: genes, proteins, and therapy. *Physiol. Rev. 81* (2), 741–66.
(22) Lansbury, P. T., and Lashuel, H. A. (2006) A century-old debate on protein aggregation and neurodegeneration enters the clinic. *Nature 443* (7113), 774–9.
(23) Jarrett, J. T., Berger, E. P., and Lansbury, P. T., Jr. (1993) The carboxy terminus of the beta amyloid protein is critical for the seeding of amyloid formation: implications for the pathogenesis of Alzheimer's disease. *Biochemistry 32* (18), 4693–7.
(24) Roher, A. E., Lowenson, J. D., Clarke, S., Wolkow, C., Wang, R., Cotter, R. J., Reardon, I. M., Zurcher-Neely, H. A., Heinrikson, R. L., Ball, M. J., et al. (1993) Structural alterations in the peptide backbone of beta-amyloid core protein may account for its deposition and stability in Alzheimer's disease. *J. Biol. Chem. 268* (5), 3072–83.
(25) Roher, A. E., Lowenson, J. D., Clarke, S., Woods, A. S., Cotter, R. J., Gowing, E., and Ball, M. J. (1993) beta-Amyloid-(1–42) is a major component of cerebrovascular amyloid deposits: implications for the pathology of Alzheimer disease. *Proc. Natl. Acad. Sci. U. S. A. 90* (22), 10836–40.
(26) Spillantini, M. G., Crowther, R. A., Jakes, R., Hasegawa, M., and Goedert, M. (1998) alpha-Synuclein in filamentous inclusions of Lewy bodies from Parkinson's disease and dementia with lewy bodies. *Proc. Natl. Acad. Sci. U. S. A. 95* (11), 6469–73.
(27) Conway, K. A., Lee, S. J., Rochet, J. C., Ding, T. T., Williamson, R. E., and Lansbury, P. T., Jr. (2000) Acceleration of oligomerization, not fibrillization, is a shared property of both alpha-synuclein mutations linked to early-onset Parkinson's disease: implications for pathogenesis and therapy. *Proc. Natl. Acad. Sci. U. S. A. 97* (2), 571–6.
(28) Goldberg, M. S., and Lansbury, P. T., Jr. (2000) Is there a cause-and-effect relationship between alpha-synuclein fibrillization and Parkinson's disease? *Nat. Cell Biol. 2* (7), E115–9.
(29) Masliah, E., Rockenstein, E., Veinbergs, I., Mallory, M., Hashimoto, M., Takeda, A., Sagara, Y., Sisk, A., and Mucke, L. (2000) Dopaminergic loss and inclusion body formation in alpha-synuclein mice: implications for neurodegenerative disorders. *Science 287* (5456), 1265–9.
(30) Sipe, J. D., and Cohen, A. S. (2000) Review: history of the amyloid fibril. *J. Struct. Biol. 130* (2–3), 88–98.
(31) Overk, C. R., and Masliah, E. (2014) Pathogenesis of synaptic degeneration in Alzheimer's disease and Lewy body disease. *Biochem. Pharmacol. 88* (4), 508–16.
(32) Dahlgren, K. N., Manelli, A. M., Stine, W. B., Jr., Baker, L. K., Krafft, G. A., and LaDu, M. J. (2002) Oligomeric and fibrillar species of amyloid-beta peptides differentially affect neuronal viability. *J. Biol. Chem. 277* (35), 32046–53.
(33) Zhang, Y., McLaughlin, R., Goodyer, C., and LeBlanc, A. (2002) Selective cytotoxicity of intracellular amyloid beta peptide1–42 through p53 and Bax in cultured primary human neurons. *J. Cell Biol. 156* (3), 519–29.
(34) Burre, J., Sharma, M., and Sudhof, T. C. (2015) Definition of a molecular pathway mediating alpha-synuclein neurotoxicity. *J. Neurosci. 35* (13), 5221–32.
(35) Morales, R., Moreno-Gonzalez, I., and Soto, C. (2013) Cross-seeding of misfolded proteins: implications for etiology and pathogenesis of protein misfolding diseases. *PLoS Pathog. 9* (9), e1003537.
(36) Miller, Y., Ma, B., and Nussinov, R. (2011) Synergistic interactions between repeats in tau protein and Abeta amyloids may be responsible for accelerated aggregation via polymorphic states. *Biochemistry 50* (23), 5172–81.
(37) Raz, Y., and Miller, Y. (2013) Interactions between Abeta and mutated Tau lead to polymorphism and induce aggregation of Abeta-mutated tau oligomeric complexes. *PLoS One 8* (8), e73303.
(38) Berhanu, W. M., Yasar, F., and Hansmann, U. H. (2013) In silico cross seeding of Abeta and amylin fibril-like oligomers. *ACS Chem. Neurosci. 4* (11), 1488–500.
(39) Luhrs, T., Ritter, C., Adrian, M., Riek-Loher, D., Bohrmann, B., Dobeli, H., Schubert, D., and Riek, R. (2005) 3D structure of Alzheimer's amyloid-beta(1–42) fibrils. *Proc. Natl. Acad. Sci. U. S. A. 102* (48), 17342–7.
(40) Petkova, A. T., Ishii, Y., Balbach, J. J., Antzutkin, O. N., Leapman, R. D., Delaglio, F., and Tycko, R. (2002) A structural model for Alzheimer's beta -amyloid fibrils based on experimental constraints from solid state NMR. *Proc. Natl. Acad. Sci. U. S. A. 99* (26), 16742–7.
(41) Atsmon-Raz, Y., and Miller, Y. (2015) A Proposed Atomic Structure of the Self-Assembly of the Non-Amyloid-beta Component of Human alpha-Synuclein As Derived by Computational Tools. *J. Phys. Chem. B 119* (31), 10005–15.
(42) Masel, J., Jansen, V. A., and Nowak, M. A. (1999) Quantifying the kinetic parameters of prion replication. *Biophys. Chem. 77* (2–3), 139–52.
(43) Stamm, M., Staritzbichler, R., Khafizov, K., and Forrest, L. R. (2014) AlignMe–a membrane protein sequence alignment web server. *Nucleic Acids Res. 42*, W246–51.

DOI: 10.1021/acschemneuro.5b00204
ACS Chem. Neurosci. 2016, 7, 46–55

(44) Stamm, M., Staritzbichler, R., Khafizov, K., and Forrest, L. R. (2013) Alignment of helical membrane protein sequences using AlignMe. *PLoS One 8* (3), e57731.
(45) Khafizov, K., Staritzbichler, R., Stamm, M., and Forrest, L. R. (2010) A study of the evolution of inverted-topology repeats from LeuT-fold transporters using AlignMe. *Biochemistry 49* (50), 10702−13.
(46) Lee, M. S., Feig, M., Salsbury, F. R., Jr., and Brooks, C. L., 3rd (2003) New analytic approximation to the standard molecular volume definition and its application to generalized Born calculations. *J. Comput. Chem. 24* (11), 1348−56.
(47) Lee, M. S., Salsbury, F. R., and Brooks, C. L. (2002) Novel generalized Born methods. *J. Chem. Phys. 116* (24), 10606.
(48) Miller, Y., Ma, B., and Nussinov, R. (2011) The unique Alzheimer's beta-amyloid triangular fibril has a cavity along the fibril axis under physiological conditions. *J. Am. Chem. Soc. 133* (8), 2742−8.
(49) Miller, Y., Ma, B., and Nussinov, R. (2010) Polymorphism in Alzheimer Abeta amyloid organization reflects conformational selection in a rugged energy landscape. *Chem. Rev. 110* (8), 4820−38.
(50) Wineman-Fisher, V., Atsmon-Raz, Y., and Miller, Y. (2015) Orientations of residues along the beta-arch of self-assembled amylin fibril-like structures lead to polymorphism. *Biomacromolecules 16* (1), 156−65.
(51) Krieger, F., Moglich, A., and Kiefhaber, T. (2005) Effect of proline and glycine residues on dynamics and barriers of loop formation in polypeptide chains. *J. Am. Chem. Soc. 127* (10), 3346−52.
(52) Steinert, P. M., Mack, J. W., Korge, B. P., Gan, S. Q., Haynes, S. R., and Steven, A. C. (1991) Glycine loops in proteins: their occurrence in certain intermediate filament chains, loricrins and single-stranded RNA binding proteins. *Int. J. Biol. Macromol. 13* (3), 130−9.
(53) Baram, M., Atsmon-Raz, Y., Ma, B., Nussinov, R., and Miller, Y. (2015) Amylin-Abeta oligomers at atomic resolution using molecular dynamics simulations: a link between Type 2 diabetes and Alzheimer's disease. *Phys. Chem. Chem. Phys.*, DOI: 10.1039/C5CP03338A.
(54) Yamazaki, T., Blinov, N., Wishart, D., and Kovalenko, A. (2008) Hydration effects on the HET-s prion and amyloid-beta fibrillous aggregates, studied with three-dimensional molecular theory of solvation. *Biophys. J. 95* (10), 4540−8.
(55) Massi, F., and Straub, J. E. (2003) Structural and dynamical analysis of the hydration of the Alzheimer's beta-amyloid peptide. *J. Comput. Chem. 24* (2), 143−53.
(56) Ma, B., and Nussinov, R. (2006) Simulations as analytical tools to understand protein aggregation and predict amyloid conformation. *Curr. Opin. Chem. Biol. 10* (5), 445−52.
(57) Clinton, L. K., Blurton-Jones, M., Myczek, K., Trojanowski, J. Q., and LaFerla, F. M. (2010) Synergistic Interactions between Abeta, tau, and alpha-synuclein: acceleration of neuropathology and cognitive decline. *J. Neurosci. 30* (21), 7281−9.
(58) Tsigelny, I. F., Crews, L., Desplats, P., Shaked, G. M., Sharikov, Y., Mizuno, H., Spencer, B., Rockenstein, E., Trejo, M., Platoshyn, O., Yuan, J. X., and Masliah, E. (2008) Mechanisms of hybrid oligomer formation in the pathogenesis of combined Alzheimer's and Parkinson's diseases. *PLoS One 3* (9), e3135.
(59) Ono, K., Takahashi, R., Ikeda, T., and Yamada, M. (2012) Cross-seeding effects of amyloid beta-protein and alpha-synuclein. *J. Neurochem. 122* (5), 883−90.
(60) Atwood, C. S., Obrenovich, M. E., Liu, T., Chan, H., Perry, G., Smith, M. A., and Martins, R. N. (2003) Amyloid-beta: a chameleon walking in two worlds: a review of the trophic and toxic properties of amyloid-beta. *Brain Res. Rev. 43* (1), 1−16.
(61) Giuffrida, M. L., Caraci, F., Pignataro, B., Cataldo, S., De Bona, P., Bruno, V., Molinaro, G., Pappalardo, G., Messina, A., Palmigiano, A., Garozzo, D., Nicoletti, F., Rizzarelli, E., and Copani, A. (2009) Beta-amyloid monomers are neuroprotective. *J. Neurosci. 29* (34), 10582−7.
(62) Bonini, N. M., and Giasson, B. I. (2005) Snaring the function of alpha-synuclein. *Cell 123* (3), 359−61.
(63) Vilar, M., Chou, H. T., Luhrs, T., Maji, S. K., Riek-Loher, D., Verel, R., Manning, G., Stahlberg, H., and Riek, R. (2008) The fold of alpha-synuclein fibrils. *Proc. Natl. Acad. Sci. U. S. A. 105* (25), 8637−42.
(64) Heise, H., Hoyer, W., Becker, S., Andronesi, O. C., Riedel, D., and Baldus, M. (2005) Molecular-level secondary structure, polymorphism, and dynamics of full-length alpha-synuclein fibrils studied by solid-state NMR. *Proc. Natl. Acad. Sci. U. S. A. 102* (44), 15871−6.
(65) Bubeck, D. (2015) Unraveling structural polymorphism of amyloid fibers. *Structure 23* (1), 10−1.
(66) Mukrasch, M. D., Bibow, S., Korukottu, J., Jeganathan, S., Biernat, J., Griesinger, C., Mandelkow, E., and Zweckstetter, M. (2009) Structural polymorphism of 441-residue tau at single residue resolution. *PLoS Biol. 7* (2), e34.
(67) Miller, Y., Ma, B., and Nussinov, R. (2009) Polymorphism of Alzheimer's Abeta17−42 (p3) oligomers: the importance of the turn location and its conformation. *Biophys. J. 97* (4), 1168−77.
(68) Hard, T. (2014) Amyloid Fibrils: Formation, Polymorphism, and Inhibition. *J. Phys. Chem. Lett. 5* (3), 607−14.
(69) Yu, X., Luo, Y., Dinkel, P., Zheng, J., Wei, G., Margittai, M., Nussinov, R., and Ma, B. (2012) Cross-seeding and conformational selection between three-and four-repeat human Tau proteins. *J. Biol. Chem. 287* (18), 14950−14959.
(70) Xiao, Y., Ma, B., McElheny, D., Parthasarathy, S., Long, F., Hoshi, M., Nussinov, R., and Ishii, Y. (2015) A[beta](1−42) fibril structure illuminates self-recognition and replication of amyloid in Alzheimer's disease. *Nat. Struct. Mol. Biol. 22* (6), 499−505.
(71) Kalé, L., Skeel, R., Bhandarkar, M., Brunner, R., Gursoy, A., Krawetz, N., Phillips, J., Shinozaki, A., Varadarajan, K., and Schulten, K. (1999) NAMD2: Greater Scalability for Parallel Molecular Dynamics. *J. Comput. Phys. 151* (1), 283.
(72) MacKerell, A. D., Bashford, D., Bellott, M., Dunbrack, R. L., Evanseck, J. D., Field, M. J., Fischer, S., Gao, J., Guo, H., Ha, S., Joseph-McCarthy, D., Kuchnir, L., Kuczera, K., Lau, F. T., Mattos, C., Michnick, S., Ngo, T., Nguyen, D. T., Prodhom, B., Reiher, W. E., Roux, B., Schlenkrich, M., Smith, J. C., Stote, R., Straub, J., Watanabe, M., Wiorkiewicz-Kuczera, J., Yin, D., and Karplus, M. (1998) All-atom empirical potential for molecular modeling and dynamics studies of proteins. *J. Phys. Chem. B 102* (18), 3586−616.
(73) Brooks, B. R., Bruccoleri, R. E., Olafson, B. D., States, D. J., Swaminathan, S., and Karplus, M. (1983) CHARMM: A program for macromolecular energy, minimization, and dynamics calculations. *J. Comput. Chem. 4* (2), 187−217.
(74) Mahoney, M. W., and Jorgensen, W. L. (2000) A five-site model for liquid water and the reproduction of the density anomaly by rigid, nonpolarizable potential functions. *J. Chem. Phys. 112* (20), 8910.
(75) Jorgensen, W. L., Chandrasekhar, J., Madura, J. D., Impey, R. W., and Klein, M. L. (1983) Comparison of simple potential functions for simulating liquid water. *J. Chem. Phys. 79* (2), 926.
(76) Tu, K., Tobias, D. J., and Klein, M. L. (1995) Constant pressure and temperature molecular dynamics simulation of a fully hydrated liquid crystal phase dipalmitoylphosphatidylcholine bilayer. *Biophys. J. 69* (6), 2558−62.
(77) Feller, S. E., Zhang, Y., Pastor, R. W., and Brooks, B. R. (1995) Constant pressure molecular dynamics simulation: The Langevin piston method. *J. Chem. Phys. 103* (11), 4613.
(78) Darden, T., York, D., and Pedersen, L. (1993) Particle mesh Ewald: An N [center-dot] log(N) method for Ewald sums in large systems. *J. Chem. Phys. 98* (12), 10089−10092.
(79) Essmann, U., Perera, L., Berkowitz, M. L., Darden, T., Lee, H., and Pedersen, L. G. (1995) A smooth particle mesh Ewald method. *J. Chem. Phys. 103* (19), 8577.
(80) Ryckaert, J.-P., Ciccotti, G., and Berendsen, H. J. C. (1977) Numerical integration of the cartesian equations of motion of a system with constraints: molecular dynamics of n - alkanes. *J. Comput. Phys. 23* (3), 327.
(81) Akesson, B., Panagiotidis, G., Westermark, P., and Lundquist, I. (2003) Islet amyloid polypeptide inhibits glucagon release and exerts a dual action on insulin release from isolated islets. *Regul. Pept. 111* (1−3), 55−60.

DOI: 10.1021/acschemneuro.5b00204
ACS Chem. Neurosci. 2016, 7, 46−55